

# BD+15 2940 AND HD 233604: TWO GIANTS WITH PLANETS CLOSE TO THE ENGULFMENT ZONE

G. NOWAK<sup>1</sup>, A. NIEDZIELSKI<sup>1</sup>, A. WOLSZCZAN<sup>2,3</sup>, M. ADAMÓW<sup>1</sup>, G. MACIEJEWSKI<sup>1</sup>

*Draft version April 26, 2013*

## ABSTRACT

We report the discovery of planetary-mass companions to two red giants by the ongoing Penn State - Toruń Planet Search (PTPS) conducted with the 9.2-m Hobby-Eberly Telescope. The 1.1 M<sub>☉</sub> K0-giant, BD+15 2940, has a 1.1 M<sub>J</sub> minimum mass companion orbiting the star at a 137.5-day period in a 0.54 AU orbit what makes it the closest - in planet around a giant and possible subject of engulfment as the consequence of stellar evolution. HD 233604, a 1.5 M<sub>☉</sub> K5-giant, is orbited by a 6.6 M<sub>J</sub> minimum mass planet which has a period of 192 days and a semi-major axis of only 0.75 AU making it one of the least distant planets to a giant star. The chemical composition analysis of HD 233604 reveals a relatively high <sup>7</sup>Li abundance which may be a sign of its early evolutionary stage or recent engulfment of another planet in the system.

We also present independent detections of planetary-mass companions to HD 209458 and HD 88133, and stellar activity-induced RV variations in HD 166435, as part of the discussion of the observing and data analysis methods used in the PTPS project.

*Subject headings:* planetary systems-stars: individual (BD+15 2940, HD 233604, HD 209458, HD 88133, HD 166435)

## 1. INTRODUCTION

A precision of the radial velocity (RV) technique, which is the most prolific ground based method of planet detection, depends on the presence of a large number of narrow spectral lines in the stellar spectra. This limits its efficiency to slowly rotating, cool stars of late-F to M spectral types which also sets an upper limit of  $M_{\star} \lesssim 1.5 M_{\odot}$  to the masses of Main Sequence (MS) target stars that may be hosts to planetary companions. Fortunately, as these stars evolve off the MS and become red giants, they cool and slow down their rotation which makes them suitable again for precision RV measurements. Despite the fact that the precision of this technique is seriously affected by stellar activity (Queloz et al. 2001) which is particularly true in the case of giant stars (Carney et al. 2003; Setiawan et al. 2004), it remains most efficient in searches for planets around A-F stars with masses as high as 5 M<sub>☉</sub>. This offers an excellent opportunity to improve our understanding of the population of planets around evolved stars that are significantly more massive than the Sun.

Searches for planets around red giants also represent an essential extension of the traditional surveys, because each detection of a planetary system around a sufficiently evolved giant provides a snapshot of the changes in its dynamical configuration powered by the evolution of the parent star. In principle, this makes it possible to track the evolution of planetary systems back to

their origins (Adamów et al. 2012) and to extrapolate it beyond the red giant stage (Villaver and Livio 2007; Mustill and Villaver 2012).

Over a dozen stars with planetary-mass companions have already been discovered by the Penn State-Toruń Centre for Astronomy Planet Search (PTPS), whose primary, long-term goal is to improve our understanding of the evolution of planetary systems around aging stars (Niedzielski et al. 2007, 2009a,b; Gettel et al. 2012b,a). Our findings are part of the growing body of discoveries by surveys such as the McDonald Observatory Planet Search (Cochran and Hatzes 1993; Hatzes and Cochran 1993), Okayama Planet Search (Sato et al. 2003), Tautenburg Planet Search (Hatzes et al. 2005), Lick K-giant Survey (Frink et al. 2002), ESO FEROS planet search (Setiawan et al. 2003), Retired A Stars and Their Companions (Johnson et al. 2007), CORALIE & HARPS search (Lovis and Mayor 2007), Boyunsen Planet Search (Omiya et al. 2011), and several others.

The existing population of planets around evolved intermediate-mass stars, uncovered by these surveys, begins to show its distinction from that of the solar type MS dwarfs. For example, the planet frequency-stellar metallicity correlation observed for MS dwarfs (Fischer and Valenti 2005) appears to be weaker in the case of planets around giants (Pasquini et al. 2007; Hekker and Meléndez 2007; Ghezzi et al. 2010), and, compared to dwarfs, the frequency of intermediate-mass stars with planets seems to be higher (Lovis and Mayor 2007; Johnson et al. 2010a, 2011). Moreover, the intermediate mass stars prefer to have more massive planets and are deficient in low mass ( $\leq 1.5 M_{\text{J}}$ ) companions (Sato et al. 2007; Niedzielski et al. 2009b; Bowler et al. 2010). Also intriguing is the growing population of brown dwarfs orbiting these stars (e.g. Liu et al. 2008; Niedzielski et al. 2009b; Quirrenbach 2011).

The most dramatic evidence for the dynamical changes in planetary systems around evolved stars has been pro-

<sup>1</sup> Toruń Center for Astronomy, Nicolaus Copernicus University, ul. Gagarina 11, 87-100 Toruń, Poland, grzegorz.nowak@astri.umk.pl, andrzej.niedzielski@astri.umk.pl, monika.adamow@astri.umk.pl, gracjan.maciejewski@astri.umk.pl

<sup>2</sup> Department of Astronomy and Astrophysics, the Pennsylvania State University, 525 Davey Laboratory, University Park, PA 16802, alex@astro.psu.edu

<sup>3</sup> Center for Exoplanets and Habitable Worlds, the Pennsylvania State University, 525 Davey Laboratory, University Park, PA 16802

vided by the observed absence of planets in orbits with semi-major axes smaller than 0.78 AU (Johnson et al. 2007). This particular property of planets around red giants detected so far seems to be an imprint of stellar evolution on planetary systems architectures. Namely, the planets at small orbital separations will tidally interact with their host stars already during their MS lifetime, and some of them will likely end up spiraling into their envelopes (see e.g. Jackson et al. 2009). However, the more distant planets, which have survived the MS evolution, may face the similar fate, when their parent stars ascend the RGB and their tidal influence extends a large distance beyond the stellar radius (Villaver and Livio 2009).

A deficit of massive planets with short orbital periods was first noted by Zucker and Mazeh (2002). The planet shortage in the separation range of 0.08-0.6 AU was explained by Udry et al. (2003) as a signature of a transition region between two categories of planets that have experienced different migration scenarios. The gap in semi-major axis distribution for planets around  $M \geq 1.2 M_{\odot}$  stars was considered by Burkert and Ida (2007) who showed that the deficiency of close-in companions to giants may reflect the dearth of 0.1-0.6 AU companions to  $M_{\star} \geq 1.2 M_{\odot}$  F-dwarfs caused by a shorter viscous diffusion timescale of their protoplanetary disks. Currie (2009) has shown through a series of Monte Carlo simulations that a stellar-mass-dependent gas disk lifetime can explain a shortage of planets with  $a < 0.5$  AU around massive stars.

Paucity of planets orbiting clump giants within  $q = a(1-e) = 0.68$  AU periastron distance was first noted by Sato et al. (2008). These authors singled out the planet engulfment at the tip of the RGB as the mechanism responsible for it. Villaver and Livio (2009) have shown that the evolution of the star alone can quantitatively explain the observed absence of close-in planets around evolved stars, when tidal interaction is taken into account. They have also provided the minimum orbital radii inside of which planets would be engulfed by stars of various masses at the end of the RGB evolution. These authors also found out that the more massive the planet, the earlier it will be captured by the stellar envelope. Nordhaus et al. (2010) studied in detail  $1 M_{\odot}$  star evolution from the ZAMS to the end of the post-MS phase and discussed the influence of tidal and mass-loss laws on the period gaps in orbits of 1, 10 and 100  $M_J$  companions. Finally, Kunitomo et al. (2011) found that minimum orbital radii are sensitive to stellar mass in the range 1.7-2.1  $M_{\odot}$  and that all the known planets indeed orbit GK clump giants beyond these survival limits, in agreement with the planet-engulfment hypothesis. These authors note, however, that planets around stars more massive than 2.1  $M_{\odot}$  have semi-major axes that are significantly larger than the minimum value, and suggest that engulfment may not be the main reason for the observed lack of short-period giant planets.

In this paper, we present the discovery of a planet that orbits its parent star just inside the currently established  $\sim 0.6$  AU "zone of avoidance", and another one that has the orbital radius that is significantly smaller than 1 AU. We also describe in some detail the method of data analysis that we have developed over the duration of the PTPS project and the RV measurements of two test stars with

known planets.

In Section 2 we describe our observing setup and give parameters of the stars discussed here. In Section 3 we present the method of data analysis and discussion of the long term stability of the HET/HRS data acquisition. The analysis of RV measurements of BD+15 2940 and HD 233604 is given in Section 4, followed by the accompanying analysis of rotation and stellar activity indicators in Section 5. Finally, our results are summarized and further discussed in Section 6.

## 2. OBSERVATIONS AND STELLAR PARAMETERS

Observations presented in this paper were made with the Hobby-Eberly Telescope (HET) (Ramsey et al. 1998) equipped with the High Resolution Spectrograph (HRS) (Tull 1998) in the queue scheduled mode (Shetrone et al. 2007). The configuration and observing procedure employed in our program were identical to those described by Cochran et al. (2004). The spectrograph, fed with the 2 arcsec fiber, was used in the  $R = 60,000$  resolution mode with a gas cell ( $I_2$ ) inserted into the optical path.

The spectra consisted of 46 echelle orders recorded on the "blue" CCD chip (407.6-592 nm) and 24 orders on the "red" one (602-783.8 nm). The spectral data used for RV measurements were extracted from the 17 orders, which cover the 505 to 592 nm range of the  $I_2$  cell spectrum. The spectra were reduced with the dedicated IRAF/Python pipeline.

### 2.1. BD+15 2940

BD+15 2940 (HIC 78407) is a  $V_T = 9.185 \pm 0.024$ ,  $B - V = 1.006 \pm 0.036$  (van Leeuwen 2007) K0 (Cannon and Pickering 1924) star in Serpens. Its Hipparcos parallax  $\pi = 1.71 \pm 1.33$  points to a distance of 585 pc. The star belongs to the PTPS Red Clump Giants sample (Zieliński et al. 2012). We collected 38 spectra of BD+15 2940 over 2362 days between 2005 March 23 and 2011 September 10 (MJD 53452-55814). The signal-to-noise ratio per resolution element (S/N) in the spectra was 120-330 at 594 nm in 316-919 seconds of integration, depending on the atmospheric conditions.

### 2.2. HD 233604

HD 233604 (BD+54 1280) is  $V_T = 10.406 \pm 0.049$  (Høg et al. 2000),  $B - V = 1.007 \pm 0.115$  (Perryman and ESA 1997), K5 (Cannon and Pickering 1924) star in Ursa Major. It belongs to the PTPS Red Clump Giant sample and it was observed at 33 epochs over the period of 2956 days from 2004 January 11 to 2012 February 14 (MJD 53015-55971). The S/N in the spectra was 110-300 at 594 nm in 762-2100 seconds of integration, depending on the atmospheric conditions.

### 2.3. HD 209458

HD 209458 (BD+18 4917, V376 Peg) a  $V_T = 7.703 \pm 0.012$ ,  $B - V = 0.594 \pm 0.015$  (van Leeuwen 2007) G0 dwarf (Montes et al. 2001), is known (Henry et al. 2000; Mazeh et al. 2000) as a host of a transiting (Charbonneau et al. 2000),  $m \sin i = 0.689 \pm 0.024 M_J$  planet at  $a = 0.04723 \pm 0.00079$  AU orbit (Butler et al. 2006) ( $P = 3.52474859 \pm 3.8 \times 10^{-7}$  d (Knutson et al. 2007)) with RV semi-amplitude of  $K = 84.67 \pm 0.7 \text{ m s}^{-1}$  (Torres et al. 2008). This star is one of the PTPS test

stars, which are known hosts to planetary systems that we have been monitoring as part of our long-term observing program. We have observed HD 209458 between 2004 July 11 and 2011 November 25 over 2693 days or 7.4 years (MJD 53197-55890) and collected 29 epochs of RV measurements. The exposure times varied between 94 and 608 seconds depending on weather conditions, typically achieving the S/N of about 200.

#### 2.4. HD 88133

HD 88133 (BD+18 2326), a  $V_T = 8.094 \pm 0.013$ ,  $B - V = 0.810 \pm 0.015$  (van Leeuwen 2007) G5 dwarf (Cannon and Pickering 1924), is another PTPS test star, a well-studied short-period host of a  $m \sin i = 0.299 \pm 0.027$   $M_J$  planet in  $a = 0.04717 \pm 0.00079$  AU ( $P = 3.41587 \pm 0.00059$  d) with the RV semi-amplitude of  $K = 36.1 \pm 3$   $\text{m s}^{-1}$  (Fischer et al. 2005; Butler et al. 2006). It was occasionally observed between 2006 January 23 and 2012 February 20 (MJD 53758-55977). 23 epochs of observations were gathered with S/N of 110-330 achieved in 141-800 seconds exposures, depending on actual weather conditions.

#### 2.5. HD 166435

HD 166435 (BD+29 3190), a  $V_T = 6.901 \pm 0.010$ ,  $B - V = 0.633 \pm 0.006$  (van Leeuwen 2007) G1 subdwarf (White et al. 2007), has been known to exhibit a pronounced stellar activity due to spots that manifests themselves as the measured RV variations induced by the line bisector variability of an amplitude of  $\sim 135$   $\text{m s}^{-1}$  (Queloz et al. 2001). As one of the PTPS test stars, it was observed between 2011 February 19 and 2011 September 22 (MJD 55611-55826) at 23 epochs. The observations resulted in S/N of 290-540 obtained with 70-700 seconds exposures, depending on actual weather conditions.

#### 2.6. Properties of the stars

The atmospheric parameters ( $T_{\text{eff}}$ ,  $\log g$ ,  $[\text{Fe}/\text{H}]$ ,  $v_{\text{micro}}$ ) of BD+15 2940 and HD 233604 were taken from Zieliński et al. (2012), who have estimated their values using the method of Takeda et al. (2002, 2005). With these values and the luminosities estimated from available data, stellar masses and ages were derived by fitting the ensemble of parameters characterizing the star ( $\log L_*/L_\odot$ ,  $\log T_{\text{eff}}$ ,  $\log g$ , and metallicity) to the evolutionary tracks of Girardi et al. (2000). The stellar radii were estimated using the derived masses and  $\log g$  from the spectroscopic analysis as described in Zieliński et al. (2012). The stellar rotation velocities of BD+15 2940 and HD 233604 were taken from Nowak et al. (2013, in preparation), who have estimated their values using the cross-correlation technique and calibrations of Fekel (1997) and Hekker and Meléndez (2007). The stellar parameters are summarized in Table 1.

For HD 209458 and HD 88133 we adopted the stellar parameters determined in Valenti and Fischer (2005) and Fischer et al. (2005), respectively.

##### 2.6.1. Li abundance

Lithium abundance analysis was performed with the Spectroscopy Made Easy package (SME, Valenti and Piskunov 1996), which requires as an input

a set of lines from the Vienna Atomic Line Database (VALD, Kupka et al. 1999) identified in the spectrum, the stellar data (including RVs), and the instrumental profile. Instead of the  $[\text{M}/\text{H}]$  ratio, also needed by the SME, the  $[\text{Fe}/\text{H}]$  values from Zieliński et al. (2012) were used as the best approximation. The 6695-6725 Å range, which covers both the  $^7\text{Li}$  line at 6708 Å and a set of Al, Ti, Si and Ca spectral lines, was modeled with the SME using the RV, rotation velocity, and macroturbulence velocity as parameters. The uncertainty of the lithium abundance estimates was derived from the rms scatter of the SME fits to all the spectra available for a given star. In addition, the analysis of lithium abundances requires a correction for non-LTE effects, especially in the case of the lithium line at 6708 Å considered here, which is affected by several non-LTE processes (Carlsson et al. 1994, and references therein). We have applied the non-LTE correction from Lind et al. (2009) to account for that effect. We have derived the values of  $A(\text{Li})$  of  $1.595 \pm 0.093$ ,  $3.104 \pm 0.056$ , and  $1.275 \pm 0.188$  for HD 88133, HD 209458 and HD 166435, respectively. Given their evolutionary status, the Li content of these stars is not abnormal. For BD+15 2940 we have measured  $A(\text{Li}) = 0.247 \pm 0.132$ , while for HD 233604  $A(\text{Li}) = 1.400 \pm 0.042$ , which makes it a Li-reach giant.

### 3. DATA ANALYSIS

#### 3.1. Radial velocity and line bisector measurements

As the HRS is a general purpose spectrograph, which is neither temperature nor pressure controlled, calibration of RV measurements with this instrument is best accomplished with the  $\text{I}_2$  cell technique. We have improved the efficiency of the entire data analysis process by combining this method (Marcy and Butler 1992; Butler et al. 1996) with that of cross-correlation (Queloz 1995; Pepe et al. 2002) for the purpose of the respective RV, line bisector span (BS) and line bisector curvature (BC) measurements in the final version of the ALICE code.

A detailed implementation of the above approach is described in Nowak (2013). Briefly, we used the  $\text{I}_2$  spectrum imprinted on the HRS flat-field spectrum to correct the initial ThAr lamp-derived wavelength scale and to determine the instrumental profile (IP) modeled as a sum of five Gaussian profiles. The wavelength scale was assumed to be linear over the 96-pixel segments that the spectra were divided into. The high S/N stellar template spectrum was then smoothed using optimal Wiener filtering (Rabiner and Gold 1975), deconvolved with the model IP using Jansson (1984) method, resampled to the corrected wavelength scale, and used as a model for RV determination from a remaining shift between the model and the stellar spectrum observed at a given epoch. The modeling process employed the non-linear least squares Levenberg-Marquardt (L-M) method (Press et al. 1992). The RV for each epoch was derived as a mean value of 391 independent measurements from the 17 usable echelle orders, after rejecting those with outlying radial velocities (more than  $3\sigma$  off the mean value) and those obtained for segments without stellar spectral lines, identified in course of cleaning the combined stellar and iodine spectra from the  $\text{I}_2$  lines. The RV uncertainty for each epoch was calculated as the error of the mean value ( $= \text{rms}/\sqrt{n_{\text{seg}}}$ ,

where  $n_{seg}$  is the number of actually used segments).

A computation of the cross-correlation functions (CCF) for the purpose of BS/BC determination was carried out as part of the above RV measurement procedure. To this end, the combined stellar and iodine spectra were first cleaned of the I<sub>2</sub> lines by dividing them by the corresponding iodine spectra imprinted in a flat-field, and then cross-correlated with a binary CCF mask. Typically the cleaned spectra and stellar template agree within 1%, consistent with the S/N ratio of 100. The mask was constructed from a synthetic K2 star spectrum of Kurucz (1993) Atlas 9 and contained about 300 lines.

The CCFs were computed in all the 17 HRS orders used for RV measurements over a wide,  $\pm 30 \text{ km s}^{-1}$  range, after correcting the spectra for their absolute radial velocity and shifting them to the Solar System barycenter (Stumpff 1980). Finally, the 17 CCFs were added together in the wavelength scale to form the integrated CCF used in further analysis. The absolute RVs at a given epoch of observations were measured from the position of a maximum of the CCF, while the CCF line bisectors and curvatures, defined in the usual way, were calculated using 3 reference ranges of (0.1 – 0.25), (0.375 – 0.525) and (0.65 – 0.8) of the central CCF intensity. The uncertainties of BS measurements were estimated with the formulae of Martínez Fiorenzano et al. (2005).

### 3.2. Modeling of radial velocity variations

We fitted Keplerian orbits to the observed RV variations using a hybrid approach (Goździewski et al. 2003; Goździewski and Migaszewski 2006; Goździewski et al. 2007), which combines the global search for a plausible range of orbital parameters with the aid of the genetic algorithm (GA), followed by a non-linear least squares or a downhill simplex fit to data to quickly converge to the preliminarily constrained  $\chi^2$  minimum.

In our implementation of this approach, once a periodic signal in a RV time series was identified in its Lomb-Scargle (L-S) periodogram (Lomb 1976; Scargle 1982), we searched for possible orbital solutions over a wide range of parameters with the PIKAIA based GA code (Charbonneau 1995). The GA semi-global search usually identified a narrow parameter range of the search space, which was then explored using the L-M algorithm to locate the best-fit Keplerian solution. In the case of a single planet the RV scrambling method (Butler et al. 2004) was used to assess the false alert probability (FAP) of the final orbital solution. If a more complicated system was indicated by a presence of two or more periodicities in the RV data, the scrambled residuals were used to quantify the goodness of the final solution. Uncertainties of the best-fit orbital parameters were estimated from either the covariance matrix of the L-M fits or from the scrambled residuals (Marcy et al. 2005).

### 3.3. Monitoring the long term stability of the HET/HRS data acquisition

Along with the target stars, we have been monitoring three stars of known RV behavior, HD 209458, HD 88133, and HD 166435, to track any possible changes in the data acquisition system that could affect the precision of RV measurements.

The RV and BS measurements for HD 209458 are listed in Table 2. The long-term RV uncertainty of  $12 \text{ m s}^{-1}$  for this star was dominated by its high  $T_{eff}$ , which resulted in a correspondingly low number of spectral lines that could be used in RV measurements. The uncertainty of the BS estimates amounted to  $38.9 \text{ m s}^{-1}$ . The L-S periodogram of the observed RV variations revealed a clear, single period of 3.52 days and no trace of any long-term trend. The best fit Keplerian model of these data is shown in Figure 1 and the corresponding orbital parameters are given in Table 5. Within uncertainties, our results are identical to those of Butler et al. (2006).

The RV and BS measurements for HD 88133 are listed in Table 3. In the case of this star, the  $6.2 \text{ m s}^{-1}$  RV uncertainty was much lower than for HD 209458, and the respective uncertainty of BS measurements was  $16.5 \text{ m s}^{-1}$ . The L-S periodogram of the RV time series exhibited a highly significant signal at a 3.41-day period, and, as in the case of HD 209458, no long-period trend. The best-fit Keplerian orbit, folded at the orbital period is presented in Figure 2 and the orbital parameters are listed in Table 5. Once again, within uncertainties, our results are identical to those of Butler et al. (2006).

Finally, despite the fact that the  $51.5 \text{ m s}^{-1}$  uncertainty of the BS measurements for HD 166435 (Table 4) was much larger than the respective RV uncertainty of  $12.7 \text{ m s}^{-1}$ , the correlation between the two quantities was obvious ( $r = 0.63$ , while the critical value of the Pearson correlation coefficient at the confidence level of 0.01 is  $r_{21,0.01} = 0.52$ , Figure 3), in agreement with the results reported by Queloz et al. (2001) for this star. This confirms the reliability of our BS measurements. Unfortunately, given the poor phase coverage of our observations we were not in position to confirm the periodic character of the RV and BS variations that mimic a planet.

Overall, the results from RV and BS monitoring of the three stars discussed above demonstrate a satisfying long-term stability of our data acquisition scheme.

## 4. RESULTS

### 4.1. BD+15 2940

RV measurements of BD+15 2940 made at 38 epochs over a period of almost 6.5 years are listed in Table 6 and shown in Figure 4. The estimated RV uncertainty for this star was  $\sigma_{RV} = 7 \text{ m s}^{-1}$  with the expected amplitude of solar-type oscillations of  $K_{osc} = 22 \text{ m s}^{-1}$  (Kjeldsen and Bedding 1995). The star exhibits RV variations with an amplitude of  $65 \text{ m s}^{-1}$  which is  $\sim 3$  times the expected RV uncertainty.

The L-S periodogram of the RV variations for this star revealed a single period of 137.5 days (Figure 6 a) and no signature of any low frequency component. The best-fit Keplerian orbit is shown in Figure 4 and its parameters are listed in Table 8. When an additional scatter  $\sigma_+$  of  $18 \text{ m s}^{-1}$  determined from this fit was added in quadrature to the original RV uncertainties, it resulted in a  $\chi^2_\nu$  value of 0.989. Note that this increase in the long-term RV uncertainty is very close to the above  $K_{osc}$  estimate and the actual jitter derived as  $\sigma_j = \sqrt{\sigma_{O-C}^2 - \sigma_{RV}^2}$ . The FAP < 0.001 for this orbital solution was estimated by performing 1000 Keplerian fits to the scrambled data points as shown in Figure 8.

Given the estimated stellar mass of  $1.1 M_{\odot}$  and the orbital period of  $P = 137.5$  days, the semi-major axis of the orbit of the planet is  $0.54$  AU, and the RV semi-amplitude of  $K = 43 \text{ m s}^{-1}$  gives its minimum mass of  $1.1 M_J$ . The moderately eccentric orbit of  $e = 0.26 \pm 0.10$  makes the planet's distance to its star vary within  $0.4$ - $0.68$  AU. Therefore, the BD+15 2940 planet is the closest one to a giant star detected so far by means of the Doppler velocity method, and the second least-massive one of all planets orbiting giants within  $1$  AU after BD+48 738 b (Gettel et al. 2012b).

#### 4.2. HD 233604

Radial velocities of HD 233604 (BD+54 1280) measured at 33 epochs over the period of 2956 days (over 8 years) are listed in Table 7 and presented in Figure 5. The estimated RV uncertainty for this star was  $9.0 \text{ m s}^{-1}$ , which is exactly the same as the estimated  $K_{osc}$  value. The measured RV amplitude was  $213 \text{ m s}^{-1}$  or  $\sim 17$  times the expected RV uncertainty.

The dominant feature in the periodogram of these RV data is the peak at a frequency corresponding to a 192-day period. The corresponding best-fit Keplerian orbit, presented in Table 8 and in Figure 5, gives the value of  $\chi^2_{\nu}$  of 2.76. An additional scatter of  $\sigma_{+} = 9 \text{ m s}^{-1}$  was added to the original errors to account for an unresolved RV variability that has apparently degraded the precision of RV measurements for this star. As in the previous case, the FAP of  $< 0.001$  (Figure 8) was calculated for this best-fit model. The orbital solution for HD 233604, together with its estimated mass of  $M_{\star} = 1.5 M_{\odot}$  gives a  $m \sin i = 6.6 M_J$  companion in a  $0.75$  AU, nearly circular orbit with  $e = 0.05 \pm 0.03$ .

### 5. STELLAR ACTIVITY ANALYSIS: LINE BISECTORS AND STELLAR PHOTOMETRY.

In order to verify that the observed RV periodicities are indeed caused by the Keplerian motion, we have thoroughly examined the existing photometry data in search for any periodic light variations, and performed a complete analysis of line bisectors and curvatures for stars discussed in this paper.

#### 5.1. BD+15 2940

With the estimated rotation velocity of  $v_{rot} \sin i_{\star} = 2.3 \pm 0.8 \text{ km s}^{-1}$  and the radius of  $R_{\star}/R_{\odot} = 14.7 \pm 2.8$  the expected upper limit to the rotation period of BD+15 2940 is 317 days, but it may range between 196 and 438 days. Therefore, it is important to consider possible sources of stellar activity that may result in the observed periodic RV signal. Such processes include stellar pulsations and a spot rotating with a star.

The p-mode oscillations can be excluded, because their expected amplitude and period are  $K_{osc} = 22 \text{ m s}^{-1}$  and  $P_{osc} = 0.68$  d, respectively (Kjeldsen and Bedding 1995). We do not resolve such the fast oscillation with our sampling that is focused on long-term RV variations. Consequently, this effect only contribute a RV-jitter to our measurements.

The mean values of the BS and the BC for this star are  $-5 \pm 23 \text{ m s}^{-1}$ , and  $-20 \pm 32 \text{ m s}^{-1}$ , respectively, with the corresponding uncertainties of  $18 \text{ m s}^{-1}$  and  $24 \text{ m s}^{-1}$ . The BS and BC amplitudes are  $45 \text{ m s}^{-1}$  and  $75 \text{ m s}^{-1}$ .

Neither BS (Figure 6 c) nor BC show any periodic signal above the  $f_n = 0.01$  level. Pearson's correlation coefficients for RV and BS and BC are 0.12 and 0.17, respectively, with the critical value at the confidence level of 0.01 is  $r_{36,0.01} = 0.41$ .

Two archival photometry datasets are available for BD+15 2940. The existing Hipparcos photometry (Perryman and ESA 1997) includes 65 epochs that uniformly cover the 1159 days (3.2 years) or  $\sim 8.5$  RV periods between MJD 47904-49063, over 12 years earlier than our RV data. No periodic signal is present in these data, either. The 362 epochs of ASAS photometry (Pojmanski 1997) collected between MJD 52685-55089 cover  $\sim 6.5$  years (2404 days) or  $\sim 12$  RV periods. These measurements, clumped in 7 groups, are contemporaneous with  $\sim 70\%$  of our RV data. Again, no trace of a periodicity is present in these data (see Figure 6 d).

Since the ASAS photometric uncertainty of  $\sigma = 0.015$  mag is typical given the observed brightness of the star, it is unlikely that it may be a noise caused by a stellar spot. However, if we made such an assumption and postulated a rotating spot that covers 1.5% of the stellar surface, the expected semi-amplitudes of RV and BS variations would be  $61$ - $95 \text{ m s}^{-1}$  and  $12$ - $19 \text{ m s}^{-1}$ , respectively, depending on the assumed model (Saar and Donahue 1997; Hatzes 2002; Desort et al. 2007). Although these values are in a reasonable agreement with our RV and BS data, there is no periodicity in the ASAS data gathered over  $\sim 12$  RV periods, and no correlation between our RV and BS measurements. Adding to these results a moderate eccentricity of the assumed Keplerian orbit, we can practically rule out a possibility that the observed RV periodicity is caused by any of the stellar phenomena discussed above and is most likely the effect of an orbital motion of a substellar mass companion to the star.

#### 5.2. HD 233604

The estimated upper limit to the rotation period of HD 233604 is 282 days and it is fairly close to the observed period of the RV variations of this star. Given the uncertainty in stellar radius and the precision of rotation velocity determination, the rotation period may range from 181 to 383 days. Obviously, it is critically important to examine the available data for a possible alternative explanation of the periodic RV signal.

Due to the length of the period of the observed RV variations and their high amplitude we can confidently reject p-mode oscillations as a cause of the RV periodicity. The most likely alternative is a spot on the stellar surface moving with the star at its rotation period. Such a spot should be detectable in both the photometric and the line profile variations.

The amplitudes and mean values of the BS and BC measurements for this star are  $65 \text{ m s}^{-1}$  and  $9.6 \pm 30.1 \text{ m s}^{-1}$ , and  $52 \text{ m s}^{-1}$  and  $-9.7 \pm 32.3 \text{ m s}^{-1}$ , respectively, and the corresponding uncertainties are 22 and  $30 \text{ m s}^{-1}$ . Neither BS (Figure 7 c) nor BC variations show any evidence for a periodicity in the computed LS periodograms. Similarly, no correlations between the RV and the BS and BC variability were found. The respective Pearson's correlation coefficients are  $r = 0.34$  for the BS and  $r = 0.20$  for the BC (with critical value of  $r_{36,0.01} = 0.44$  for the confidence level of 0.01).

In the case of this star, long-term photometric time se-

ries are available from the NSVS (Woźniak et al. 2004) and the WASP (Pollacco et al. 2006). SWASP photometry consists of 2767 measurements between MJD 54189 and 54575, which are contemporaneous with our spectroscopic observations but cover only a small part of their time baseline. In fact, most of the available epochs of photometry fall within 175 days between MJD 54400 through MJD 54575. The NSVS photometry is of a better quality and consists of 309 measurements made between MJD 51272 and MJD 51633, which amounts to 361 days of data collected about 4 years earlier than our HET observations. These data are clustered in two groups, each covering a fraction of the orbital period.

The LS analysis reveals no periodic signal in SWASP data, but four significant periodicities are found in the NSVS photometry with  $f_n < 0.001$ . Two of them that are close to a 1-day period are most likely artifacts of the particular cadence of the RV observations. Two other two at 28.1 and 27.7 days are most likely caused by the residual lunar illumination of the field that was not removed in the photometric data reduction process.

As in the case of BD+15 2940, we can make a very conservative assumption that the SWASP photometric uncertainty of  $\sigma = 0.018$  mag is caused by a spot, covering 1.8% of the stellar surface. This gives the expected semi-amplitude of RV and BS variations of  $70\text{--}111\text{ ms}^{-1}$  and  $13\text{--}20\text{ ms}^{-1}$ , respectively, depending on the assumed model (Saar and Donahue 1997; Hatzes 2002; Desort et al. 2007). The expected RV variations estimated under such an unfavorable assumption are 1.6–2.5 times smaller than those observed.

Altogether, the absence of the periodicity seen in the RV data in the available photometric data, and no correlation between BC, BS and RV variations make it unlikely that they are induced by stellar activity. An additional evidence supporting the Keplerian origin of the observed periodic RV variations is provided by the fact that they are much larger than expected under the assumption that the photometric data scatter is dominated by a rotating spot on the stellar surface.

## 6. DISCUSSION

In this paper we have presented the detection of two planetary-mass companions to two red giants in the solar to intermediate-mass range. HD 233604 hosts a  $m \sin i = 6.6\text{ M}_J$  planet in a 0.75 AU or  $\sim 15 R_*$  orbit. The planet’s closest approach to the star at the periastron distance of  $q$  is 0.71 AU or  $\sim 14$  stellar radii. BD+15 2940 harbors a  $m \sin i = 1.1\text{ M}_J$  planet in a 0.54 AU or only  $\sim 7.9 R_*$  orbit which approaches the star as close as  $q = 0.4$  AU or  $\sim 5.8 R_*$ . Both giants belong to the Red Giant Clump and, given a large uncertainty in their luminosity determinations, their exact evolutionary stages and ages are not known. They are most likely evolving upwards the red giant branch toward the helium-flash, but their location on the horizontal branch cannot be excluded.

The case of the  $M_* = 1.5\text{ M}_\odot$  star, HD 233604, is of special interest, as this giant exhibits a relatively high Li abundance. This suggests that the star is still before the first dredge-up process (Iben 1967b). Alternatively, but less likely, it may be another case of a recent engulfment episode similar to that of BD+48 740 (Adamów et al. 2012). The more likely pre-dredge-up scenario would mean that the HD 233604 planetary system was not yet

affected by a substantial stellar radius growth before the helium flash and the subsequent severe mass-loss. The low rotation velocity of HD 233604 additionally supports this scenario. A more detailed, ongoing chemical composition study will allow constraining the evolutionary status of this star much better.

The status of the  $M_* = 1.1\text{ M}_\odot$  star, BD+15 2940, is less certain. Its poorly determined but definitely relatively high luminosity suggests that the star is a rather evolved, He-burning object already past the episode of stellar radius expansion.

A useful way to illustrate the occurrence of tight-orbit planets around various types of stars is to plot their semi-major-axes against the values of the stellar  $\log g$ . Such a plot of the current catalog of 778 planets (Schneider et al. 2011) is shown in Figure 9. Clearly, the most recent data show that there are no planets within the borderline of  $\log(a[\text{AU}]) = -0.633 \log g + 0.975$  (set by HD 96127 b and Kepler-10 b positions in that graph). The only exception is the intriguing system of HIP 13044 (Setiawan et al. 2010).

Planets over the whole range of orbital separations, all the way down to Hot Jupiters, can be found around MS stars with  $4 < \log g \leq 5$ . Also, sub-giant ( $\log g \sim 3.5$ ) companions still cover a wide range of orbital radii, with the current lower limit of 0.0810 AU in the case of HD 102956 (Johnson et al. 2010b), but, interestingly, there are very few planets inside 1 AU of these stars. In particular none is known within  $0.08\text{ AU} < a < 0.76\text{ AU}$  in accordance with the predictions of (Burkert and Ida 2007).

Planets in orbits around more evolved stars with even lower  $\log g \sim 2\text{--}3$  are indeed found outside the predicted borderline, as illustrated by the 0.54 AU orbit of the BD+15 2940 planet discussed here. However, one notes that planets around giants are generally found in tighter orbits than those around sub-giants (except HD 102956 b). This suggests that, in addition to the absence of 0.1–0.6 AU companions to  $M_* \geq 1.2\text{ M}_\odot$  F dwarfs, another effect must influence the orbits of planets around those evolved stars. This effect has been identified as the tidal interaction between the star and the planet, which may cause an accelerated orbital decay (Rasio et al. 1996; Villaver and Livio 2009). According to Villaver and Livio (2009), a  $2\text{ M}_\odot$  star, a typical object in the observed population within the  $\log g \sim 2\text{--}3$  range, should have already ingested 3–5  $\text{M}_J$  or more massive planets in orbits up to 0.2 AU before reaching  $\log L_*/L_\odot = 2$  (or  $\log g \sim 2.3$ ) on the Red Giant Branch.

Both HD 233604 b and BD+15 2940 b fall into that part of Figure 9 as well. However, HD 233604 b in 0.75 AU or of  $q = 0.71$  AU orbit around its  $M_* = 1.5\text{ M}_\odot$  host is located well within the minimum orbital radius as defined in Villaver and Livio (2009) and Kunitomo et al. (2011) for a Jupiter mass planet. With the estimated  $M_* = 1.1\text{ M}_\odot$  BD+15 2940 planet in 0.54 AU or only  $q = 0.4$  AU is located even closer, within the star’s RGB tip radius (Villaver and Livio 2009). Existence of such close-in planets suggests that the influence of star-planet tidal interactions in late stages of stellar evolution may be overestimated. The relatively large eccentricity,  $e = 0.26 \pm 0.1$ , of the BD+15 2940 planet also deserves more attention as one might expect its orbit to be already circularized at the distance of only 5.8 stellar radii from

the star. On the other hand, it may represent a reminiscence of a recent planet-planet interaction in the system (Voyatzis et al. 2013).

Even more evolved hosts of planetary systems, with  $\log g < 2$ , form a very heterogeneous group with masses ranging from around  $1 M_{\odot}$  (42 Dra) up to  $M_{\star} = 4.5 M_{\odot}$  (HD 13189). As the evolution of planetary systems affected by tidal interactions and mass loss is very much stellar mass-dependent, it is difficult to discuss them together. These stars also exhibit substantial amounts of variability characterized by post-fit RV rms values easily reaching  $55\text{--}60 \text{ m s}^{-1}$  (Hatzes et al. 2005; Niedzielski et al. 2007) which makes studying them even more difficult.

Although the population of planetary systems detected around evolved stars has been steadily growing, it is still too meager to achieve satisfying levels of understanding of the star-planetary system interaction driven by the post-MS stellar evolution. An additional, important complication stems from the fact that luminosities of these stars are typically poorly determined, which obviously makes constraining their evolutionary status very difficult. In any case, continuing studies of such systems provide important contributions to the process of creating a general picture of the evolution of planetary systems under the influence of their evolving parent stars.

We thank Dr. Nikolai Piskunov for making SME available for us. We thank the HET resident astronomers and telescope operators for continuous support. GN, AN and MA were supported by the Polish Ministry of Science and Higher Education grant N N203 510938. GN acknowledges support from Polish Ministry of Science and Higher Education grant N N203 386237. AW was supported by the NASA grant NNX09AB36G. The HET is a joint project of the University of Texas at Austin, the Pennsylvania State University, Stanford University, Ludwig-Maximilians-Universität München, and Georg-August-Universität Göttingen. The HET is named in honor of its principal benefactors, William P. Hobby and Robert E. Eberly. The Center for Exoplanets and Habitable Worlds is supported by the Pennsylvania State University, the Eberly College of Science, and the Pennsylvania Space Grant Consortium. This research has made extensive use of the SIMBAD database, operated at CDS (Strasbourg, France) and NASA’s Astrophysics Data System Bibliographic Services. This research has made use of the The Extrasolar Planets Encyclopaedia at [exoplanet.eu](http://exoplanet.eu).

## REFERENCES

- Adamów, M., Niedzielski, A., Villaver, E., Nowak, G., and Wolszczan, A.: 2012, *ApJ* **754**, L15
- Bowler, B. P., Johnson, J. A., Marcy, G. W., Henry, G. W., Peek, K. M. G., Fischer, D. A., Clubb, K. I., Liu, M. C., Reffert, S., Schwab, C., and Lowe, T. B.: 2010, *ApJ* **709**, 396
- Burkert, A. and Ida, S.: 2007, *ApJ* **660**, 845
- Butler, R. P., Marcy, G. W., Williams, E., McCarthy, C., Dosanji, P., and Vogt, S. S.: 1996, *PASP* **108**, 500
- Butler, R. P., Vogt, S. S., Marcy, G. W., Fischer, D. A., Wright, J. T., Henry, G. W., Laughlin, G., and Lissauer, J. J.: 2004, *ApJ* **617**, 580
- Butler, R. P., Wright, J. T., Marcy, G. W., Fischer, D. A., Vogt, S. S., Tinney, C. G., Jones, H. R. A., Carter, B. D., Johnson, J. A., McCarthy, C., and Penny, A. J.: 2006, *ApJ* **646**, 505
- Cannon, A. J. and Pickering, E. C.: 1924, *Henry Draper (HD) catalog and HD extension*
- Carlsson, M., Rutten, R. J., Bruls, J. H. M. J., and Shchukina, N. G.: 1994, *A&A* **288**, 860
- Carney, B. W., Latham, D. W., Stefanik, R. P., Laird, J. B., and Morse, J. A.: 2003, *AJ* **125**, 293
- Charbonneau, D., Brown, T. M., Latham, D. W., and Mayor, M.: 2000, *ApJ* **529**, L45
- Charbonneau, P.: 1995, *ApJS* **101**, 309
- Cochran, W. D., Endl, M., McArthur, B., Paulson, D. B., Smith, V. V., MacQueen, P. J., Tull, R. G., Good, J., Booth, J., Shetrone, M., Roman, B., Odewahn, S., Deglman, F., Graver, M., Soukup, M., and Villarreal, Jr., M. L.: 2004, *ApJ* **611**, L133
- Cochran, W. D. and Hatzes, A. P.: 1993, in J. A. Phillips, S. E. Thorsett, and S. R. Kulkarni (eds.), *Planets Around Pulsars*, Vol. 36 of *Astronomical Society of the Pacific Conference Series*, pp 267–273
- Currie, T.: 2009, *ApJ* **694**, L171
- Desort, M., Lagrange, A.-M., Galland, F., Udry, S., and Mayor, M.: 2007, *A&A* **473**, 983
- Fekel, F. C.: 1997, *PASP* **109**, 514
- Fischer, D. A., Laughlin, G., Butler, P., Marcy, G., Johnson, J., Henry, G., Valenti, J., Vogt, S., Ammons, M., Robinson, S., Spear, G., Strader, J., Driscoll, P., Fuller, A., Johnson, T., Manrao, E., McCarthy, C., Muñoz, M., Tah, K. L., Wright, J., Ida, S., Sato, B., Toyota, E., and Minniti, D.: 2005, *ApJ* **620**, 481
- Fischer, D. A. and Valenti, J.: 2005, *ApJ* **622**, 1102
- Frink, S., Mitchell, D. S., Quirrenbach, A., Fischer, D. A., Marcy, G. W., and Butler, R. P.: 2002, *ApJ* **576**, 478
- Gottel, S., Wolszczan, A., Niedzielski, A., Nowak, G., Adamów, M., Zieliński, P., and Maciejewski, G.: 2012a, *ApJ* **756**, 53
- Gottel, S., Wolszczan, A., Niedzielski, A., Nowak, G., Adamów, M., Zieliński, P., and Maciejewski, G.: 2012b, *ApJ* **745**, 28
- Ghezzi, L., Cunha, K., Schuler, S. C., and Smith, V. V.: 2010, *ApJ* **725**, 721
- Girardi, L., Bressan, A., Bertelli, G., and Chiosi, C.: 2000, *A&AS* **141**, 371
- Goździewski, K., Konacki, M., and Maciejewski, A. J.: 2003, *ApJ* **594**, 1019
- Goździewski, K., Maciejewski, A. J., and Migaszewski, C.: 2007, *ApJ* **657**, 546
- Goździewski, K. and Migaszewski, C.: 2006, *A&A* **449**, 1219
- Hatzes, A. P.: 2002, *Astronomische Nachrichten* **323**, 392
- Hatzes, A. P. and Cochran, W. D.: 1993, *ApJ* **413**, 339
- Hatzes, A. P., Guenther, E. W., Endl, M., Cochran, W. D., Döllinger, M. P., and Bedalov, A.: 2005, *A&A* **437**, 743
- Hekker, S. and Meléndez, J.: 2007, *A&A* **475**, 1003
- Henry, G. W., Marcy, G. W., Butler, R. P., and Vogt, S. S.: 2000, *ApJ* **529**, L41
- Høg, E., Fabricius, C., Makarov, V. V., Urban, S., Corbin, T., Wycoff, G., Bastian, U., Schwendicke, P., and Wicenec, A.: 2000, *A&A* **355**, L27
- Iben, Jr., I.: 1967b, *ApJ* **147**, 624
- Jackson, B., Barnes, R., and Greenberg, R.: 2009, *ApJ* **698**, 1357
- Jansson, P. A.: 1984, *Deconvolution. With applications in spectroscopy*
- Johnson, J. A., Aller, K. M., Howard, A. W., and Crepp, J. R.: 2010a, *PASP* **122**, 905
- Johnson, J. A., Bowler, B. P., Howard, A. W., Henry, G. W., Marcy, G. W., Isaacson, H., Brewer, J. M., Fischer, D. A., Morton, T. D., and Crepp, J. R.: 2010b, *ApJ* **721**, L153
- Johnson, J. A., Clanton, C., Howard, A. W., Bowler, B. P., Henry, G. W., Marcy, G. W., Crepp, J. R., Endl, M., Cochran, W. D., MacQueen, P. J., Wright, J. T., and Isaacson, H.: 2011, *ApJS* **197**, 26
- Johnson, J. A., Fischer, D. A., Marcy, G. W., Wright, J. T., Driscoll, P., Butler, R. P., Hekker, S., Reffert, S., and Vogt, S. S.: 2007, *ApJ* **665**, 785
- Kjeldsen, H. and Bedding, T. R.: 1995, *A&A* **293**, 87
- Knutson, H. A., Charbonneau, D., Noyes, R. W., Brown, T. M., and Gilliland, R. L.: 2007, *ApJ* **655**, 564
- Kunitomo, M., Ikoma, M., Sato, B., Katsuta, Y., and Ida, S.: 2011, *ApJ* **737**, 66
- Kupka, F., Piskunov, N., Ryabchikova, T. A., Stempels, H. C., and Weiss, W. W.: 1999, *A&AS* **138**, 119
- Kurucz, R.: 1993, *ATLAS9 Stellar Atmosphere Programs and 2 km/s grid. Kurucz CD-ROM No. 13. Cambridge, Mass.: Smithsonian Astrophysical Observatory, 1993*, 13
- Lind, K., Asplund, M., and Barklem, P. S.: 2009, *A&A* **503**, 541
- Liu, Y.-J., Sato, B., Zhao, G., Noguchi, K., Wang, H., Kambe, E., Ando, H., Izumiura, H., Chen, Y.-Q., Okada, N., Toyota, E., Omiya, M., Masuda, S., Takeda, Y., Murata, D., Itoh, Y., Yoshida, M., Kokubo, E., and Ida, S.: 2008, *ApJ* **672**, 553
- Lomb, N. R.: 1976, *ApJSS* **39**, 447
- Lovis, C. and Mayor, M.: 2007, *A&A* **472**, 657
- Marcy, G. W. and Butler, R. P.: 1992, *PASP* **104**, 270
- Marcy, G. W., Butler, R. P., Vogt, S. S., Fischer, D. A., Henry, G. W., Laughlin, G., Wright, J. T., and Johnson, J. A.: 2005, *ApJ* **619**, 570
- Martínez Fiorenzano, A. F., Gratton, R. G., Desidera, S., Cosentino, R., and Endl, M.: 2005, *A&A* **442**, 775
- Mazeh, T., Naef, D., Torres, G., Latham, D. W., Mayor, M., Beuzit, J.-L., Brown, T. M., Buchhave, L., Burnet, M., Carney, B. W., Charbonneau, D., Drukier, G. A., Laird, J. B., Pepe, F., Perrier, C., Queloz, D., Santos, N. C., Sivan, J.-P., Udry, S., and Zucker, S.: 2000, *ApJ* **532**, L55
- Montes, D., López-Santiago, J., Gálvez, M. C., Fernández-Figueroa, M. J., De Castro, E., and Cornide, M.: 2001, *MNRAS* **328**, 45
- Mustill, A. J. and Villaver, E.: 2012, *ApJ* **761**, 121
- Niedzielski, A., Goździewski, K., Wolszczan, A., Konacki, M., Nowak, G., and Zieliński, P.: 2009a, *ApJ* **693**, 276
- Niedzielski, A., Konacki, M., Wolszczan, A., Nowak, G., Maciejewski, G., Gelino, C. R., Shao, M., Shetrone, M., and Ramsey, L. W.: 2007, *ApJ* **669**, 1354
- Niedzielski, A., Nowak, G., Adamów, M., and Wolszczan, A.: 2009b, *ApJ* **707**, 768
- Nordhaus, J., Spiegel, D. S., Ibgui, L., Goodman, J., and Burrows, A.: 2010, *MNRAS* **408**, 631
- Nowak, G.: 2013, *Ph.D. Thesis*, Nicolaus Copernicus University, Toruń, Poland
- Omiya, M., Han, I., Izumiura, H., Lee, B.-C., Sato, B., Kim, K.-M., Yoon, T. S., Kambe, E., Yoshida, M., Masuda, S., Toyota, E., Urakawa, S., and Takada-Hidai, M.: 2011, in S. Schuh, H. Drechsel, and U. Heber (eds.), *American Institute of Physics Conference Series*, Vol. 1331 of *American Institute of Physics Conference Series*, pp 122–129
- Pasquini, L., Döllinger, M. P., Weiss, A., Girardi, L., Chavero, C., Hatzes, A. P., da Silva, L., and Setiawan, J.: 2007, *A&A* **473**, 979
- Pepe, F., Mayor, M., Galland, F., Naef, D., Queloz, D., Santos, N. C., Udry, S., and Burnet, M.: 2002, *A&A* **388**, 632
- Perryman, M. A. C. and ESA (eds.): 1997, *The HIPPARCOS and TYCHO catalogues. Astrometric and photometric star catalogues derived from the ESA HIPPARCOS Space Astrometry Mission*, Vol. 1200 of *ESA Special Publication*
- Pojmanski, G.: 1997, *Acta Astronomica* **47**, 467



- Pollacco, D. L., Skillen, I., Collier Cameron, A., Christian, D. J., Hellier, C., Irwin, J., Lister, T. A., Street, R. A., West, R. G., Anderson, D., Clarkson, W. I., Deeg, H., Enoch, B., Evans, A., Fitzsimmons, A., Haswell, C. A., Hodgkin, S., Horne, K., Kane, S. R., Keenan, F. P., Maxted, P. F. L., Norton, A. J., Osborne, J., Parley, N. R., Ryans, R. S. I., Smalley, B., Wheatley, P. J., and Wilson, D. M.: 2006, *PASP* **118**, 1407
- Press, W. H., Teukolsky, S. A., Vetterling, W. T., and Flannery, B. P.: 1992, *Numerical recipes in FORTRAN. The art of scientific computing*
- Queloz, D.: 1995, in A. G. D. Philip, K. Janes, & A. R. Upgren (ed.), *New Developments in Array Technology and Applications*, Vol. 167 of *IAU Symposium*, pp 221–+
- Queloz, D., Henry, G. W., Sivan, J. P., Baliunas, S. L., Beuzit, J. L., Donahue, R. A., Mayor, M., Naef, D., Perrier, C., and Udry, S.: 2001, *A&A* **379**, 279
- Quirrenbach, A.: 2011, in *AAS/Division for Extreme Solar Systems Abstracts*, Vol. 2 of *AAS/Division for Extreme Solar Systems Abstracts*, p. 2008
- Rabiner, L. R. and Gold, B.: 1975, *Theory and application of digital signal processing*
- Ramsey, L. W., Adams, M. T., Barnes, T. G., Booth, J. A., Cornell, M. E., Fowler, J. R., Gaffney, N. I., Glaspey, J. W., Good, J. M., Hill, G. J., Kelton, P. W., Krabbendam, V. L., Long, L., MacQueen, P. J., Ray, F. B., Ricklefs, R. L., Sage, J., Sebring, T. A., Spiesman, W. J., and Steiner, M.: 1998, in L. M. Stepp (ed.), *Society of Photo-Optical Instrumentation Engineers (SPIE) Conference Series*, Vol. 3352 of *Society of Photo-Optical Instrumentation Engineers (SPIE) Conference Series*, pp 34–42
- Rasio, F. A., Tout, C. A., Lubow, S. H., and Livio, M.: 1996, *ApJ* **470**, 1187
- Saar, S. H. and Donahue, R. A.: 1997, *ApJ* **485**, 319
- Sato, B., Ando, H., Kambe, E., Takeda, Y., Izumiura, H., and Masuda, S.: 2003, in D. Deming and S. Seager (eds.), *Scientific Frontiers in Research on Extrasolar Planets*, Vol. 294 of *Astronomical Society of the Pacific Conference Series*, pp 51–54
- Sato, B., Izumiura, H., Toyota, E., Kambe, E., Ikoma, M., Omiya, M., Masuda, S., Takeda, Y., Murata, D., Itoh, Y., Ando, H., Yoshida, M., Kokubo, E., and Ida, S.: 2008, *PASJ* **60**, 539
- Sato, B., Izumiura, H., Toyota, E., Kambe, E., Takeda, Y., Masuda, S., Omiya, M., Murata, D., Itoh, Y., Ando, H., Yoshida, M., Ikoma, M., Kokubo, E., and Ida, S.: 2007, *ApJ* **661**, 527
- Scargle, J. D.: 1982, *ApJ* **263**, 835
- Schneider, J., Dedieu, C., Le Sidaner, P., Savalle, R., and Zolotukhin, I.: 2011, *A&A* **532**, A79
- Setiawan, J., Klement, R. J., Henning, T., Rix, H.-W., Rochau, B., Rodmann, J., and Schulze-Hartung, T.: 2010, *Science* **330**, 1642
- Setiawan, J., Pasquini, L., da Silva, L., Hatzes, A. P., von der Lühse, O., Girardi, L., de Medeiros, J. R., and Guenther, E.: 2004, *A&A* **421**, 241
- Setiawan, J., Pasquini, L., da Silva, L., von der Lühse, O., and Hatzes, A.: 2003, *A&A* **397**, 1151
- Shetrone, M., Cornell, M. E., Fowler, J. R., Gaffney, N., Laws, B., Mader, J., Mason, C., Odewahn, S., Roman, B., Rostopchin, S., Schneider, D. P., Umbarger, J., and Westfall, A.: 2007, *PASP* **119**, 556
- Stumpff, P.: 1980, *A&AS* **41**, 1
- Takeda, Y., Ohkubo, M., and Sadakane, K.: 2002, *PASJ* **54**, 451
- Takeda, Y., Ohkubo, M., Sato, B., Kambe, E., and Sadakane, K.: 2005, *PASJ* **57**, 27
- Torres, G., Winn, J. N., and Holman, M. J.: 2008, *ApJ* **677**, 1324
- Tull, R. G.: 1998, in S. D’Odorico (ed.), *Society of Photo-Optical Instrumentation Engineers (SPIE) Conference Series*, Vol. 3355 of *Society of Photo-Optical Instrumentation Engineers (SPIE) Conference Series*, pp 387–398
- Udry, S., Mayor, M., and Santos, N. C.: 2003, *A&A* **407**, 369
- Valenti, J. A. and Fischer, D. A.: 2005, *ApJS* **159**, 141
- Valenti, J. A. and Piskunov, N.: 1996, *A&AS* **118**, 595
- van Leeuwen, F. (ed.): 2007, *Hipparcos, the New Reduction of the Raw Data*, Vol. 350 of *Astrophysics and Space Science Library*
- Villaver, E. and Livio, M.: 2007, *ApJ* **661**, 1192
- Villaver, E. and Livio, M.: 2009, *ApJ* **705**, L81
- Voyatzis, G., Hadjidemetriou, J. D., Veras, D., and Varvoglis, H.: 2013, *ArXiv e-prints*
- White, R. J., Gabor, J. M., and Hillenbrand, L. A.: 2007, *AJ* **133**, 2524
- Woźniak, P. R., Vestrand, W. T., Akerlof, C. W., Balsano, R., Bloch, J., Casperson, D., Fletcher, S., Gisler, G., Kehoe, R., Kinemuchi, K., Lee, B. C., Marshall, S., McGowan, K. E., McKay, T. A., Rykoff, E. S., Smith, D. A., Szymanski, J., and Wren, J.: 2004, *AJ* **127**, 2436
- Zieliński, P., Niedzielski, A., Wolszczan, A., Adamów, M., and Nowak, G.: 2012, *A&A* **547**, A91
- Zucker, S. and Mazeh, T.: 2002, *ApJ* **568**, L113

TABLE 1  
STELLAR PARAMETERS OF BD+15 2940 AND HD 233604.

Parameter	BD+15 2940	HD 233604
$V_T$ (mag)	$9.185 \pm 0.024$	$10.406 \pm 0.049$
$(B - V)$ (mag)	$1.006 \pm 0.036$	$1.007 \pm 0.115$
Spectral type	K0	K5
$\pi$ (mas)	$1.71 \pm 1.33$	—
$T_{eff}$ (K)	$4796 \pm 117$	$4791 \pm 45$
$\log g$	$2.8 \pm 0.45$	$2.55 \pm 0.18$
(Fe/H)	$0.28 \pm 0.07$	$-0.36 \pm 0.04$
$\log L_*/L_\odot$	$2.01 \pm 0.75$	$1.75 \pm 0.18$
$M_*/M_\odot$	$1.1 \pm 0.2$	$1.50 \pm 0.30$
$R_*/R_\odot$	$14.7 \pm 2.8$	$10.9 \pm 0.6$
Age (Gyr)	$7.1 \pm 4.2$	$2.4 \pm 1.8$
$v_{rot} \sin i_*$ (km s $^{-1}$ )	$2.3 \pm 0.8$	$2.0 \pm 0.8$
$P_{rot}(\sin i_*)^{-1}$ (days)	$317 \pm 121$	$282 \pm 111$
$K_{osc}$ (m s $^{-1}$ )	$22^{+137}_{-19}$	$9^{+9}_{-4}$
$P_{osc}$ (days)	$0.68^{+0.51}_{-0.31}$	$0.27^{+0.11}_{-0.07}$

TABLE 2  
RELATIVE RADIAL VELOCITIES AND BISECTOR SPAN OF HD 209458.

Epoch (MJD)	RV (m s $^{-1}$ )	$\sigma_{RV}$ (m s $^{-1}$ )	BS (m s $^{-1}$ )	$\sigma_{BS}$ (m s $^{-1}$ )
53197.29482	-80.9	13.1	39.9	37.3
53538.35438	-73.1	14.7	123.9	46.9
53544.34874	49.9	13.9	-11.5	37.9
53547.33435	57.4	14.5	-19.8	39.0
53984.34746	65.7	13.3	-13.6	40.3
54001.09852	-53.7	11.3	19.7	33.4
54014.26729	-34.1	9.7	3.5	36.2
54056.13726	50.6	12.1	60.2	42.9
54448.07560	-59.1	7.3	33.6	26.2
54738.09154	18.8	15.3	-0.0	52.1
54756.22903	53.4	11.2	70.3	35.9
54759.20674	-32.3	13.4	9.9	43.9
54764.21486	100.9	10.5	-18.3	44.2
54777.16241	27.9	9.5	38.0	39.3
54780.15300	-21.4	12.1	-14.0	48.3
54786.13373	-26.2	12.4	82.3	54.2
54792.13299	122.2	10.9	39.0	44.2
54813.07756	115.0	10.9	95.2	36.8
55031.26789	63.4	15.3	18.2	48.1
55068.16183	-28.8	15.0	-8.5	38.1
55110.25281	3.1	11.8	-61.2	38.6
55502.17681	-67.2	12.2	-19.0	41.8
55504.18200	96.2	9.6	-23.4	26.1
55506.18306	-60.1	9.5	9.6	28.4
55510.15573	-33.5	11.2	40.4	39.4
55510.15868	-35.6	9.2	39.7	36.5
55513.16310	-77.0	12.9	47.1	36.8
55515.15433	34.4	13.6	-47.7	29.6
55890.13839	-82.0	7.7	56.8	25.2

TABLE 3  
RELATIVE RADIAL VELOCITIES AND BISECTOR SPAN OF HD 88133.

Epoch (MJD)	RV ( $\text{m s}^{-1}$ )	$\sigma_{\text{RV}}$ ( $\text{m s}^{-1}$ )	BS ( $\text{m s}^{-1}$ )	$\sigma_{\text{BS}}$ ( $\text{m s}^{-1}$ )
53758.26950	-21.4	5.5	-28.8	14.2
53774.21259	33.2	6.0	-30.2	14.6
53835.25918	27.5	6.6	-27.5	13.4
53868.17657	-19.8	6.5	-12.8	13.8
54090.36895	-31.8	5.3	-18.4	17.6
54090.37559	-30.5	6.6	-43.0	19.8
54165.36426	-21.8	6.3	15.0	16.4
54461.34054	8.9	5.6	-32.0	15.1
54465.32153	-32.2	5.6	-13.6	13.5
54474.31236	43.2	6.2	-24.9	16.0
54767.50684	29.3	7.5	22.7	19.4
54777.48514	12.0	6.2	-41.6	20.2
54782.47424	-7.1	6.1	28.8	19.6
54785.45165	18.8	6.5	-5.3	18.8
54788.45604	29.1	5.4	9.4	16.7
54858.46134	-28.6	8.1	-11.0	21.5
54864.44610	-9.5	7.4	-12.1	19.1
55137.50172	-15.8	5.1	-8.7	14.2
55940.50047	-34.2	6.1	2.9	17.0
55948.27405	-13.6	4.7	-60.2	11.1
55956.24389	37.6	5.4	11.4	10.9
55973.40238	28.1	6.4	-9.5	18.9
55977.19226	12.5	6.3	-11.8	16.9

TABLE 4  
RELATIVE RADIAL VELOCITIES AND BISECTOR SPAN OF HD 166435.

Epoch (MJD)	RV ( $\text{m s}^{-1}$ )	$\sigma_{\text{RV}}$ ( $\text{m s}^{-1}$ )	BS ( $\text{m s}^{-1}$ )	$\sigma_{\text{BS}}$ ( $\text{m s}^{-1}$ )
55611.51710	-33.2	10.8	27.7	56.5
55612.50123	-33.4	8.4	-3.9	52.1
55613.51535	10.5	15.7	23.3	52.9
55615.51164	-24.1	16.8	-54.3	51.8
55616.50156	29.1	10.2	-47.1	58.9
55626.49751	-15.8	18.0	20.3	56.1
55627.47291	15.2	10.3	-54.4	53.9
55628.49111	12.1	18.9	-99.7	66.7
55634.45595	51.8	10.3	-104.3	55.1
55639.44095	-7.3	12.8	10.9	68.0
55640.44137	-15.3	10.2	-77.0	60.8
55643.41648	-41.3	16.4	52.0	61.4
55644.42200	46.8	15.2	-91.9	44.8
55645.40177	30.3	18.1	-92.1	63.6
55801.24069	26.1	11.0	-154.1	48.4
55805.21921	43.0	11.0	-145.8	44.6
55814.18152	-28.4	9.0	-14.6	40.2
55815.18623	-59.8	12.8	-32.5	40.5
55816.18358	34.5	11.0	-45.3	43.3
55817.18530	-1.6	11.5	-70.8	42.5
55824.15294	4.7	11.3	-18.2	41.2
55825.14860	-24.6	11.1	-28.3	42.2
55826.13646	0.2	11.5	-129.4	39.5

TABLE 5  
ORBITAL PARAMETERS OF HD 209458 B AND HD 88133 B.

Parameter	HD 209458 b	HD 88133 b
$P$ (days)	$3.525 \pm 0.009$	$3.415 \pm 0.001$
$T_0$ (MJD)	$53199.3 \pm 0.9$	$53760.7 \pm 0.9$
$K$ ( $\text{m s}^{-1}$ )	$87.7 \pm 5.4$	$34.2 \pm 3.6$
$e$	$0.007 \pm 0.060$	$0.09 \pm 0.07$
$\omega$ (deg)	$60 \pm 108$	$15 \pm 120$
$m \sin i$ ( $M_J$ )	0.714	0.284
$a$ (AU)	0.0474	0.047
$RV_0$ ( $\text{m s}^{-1}$ )	$11.1 \pm 3.4$	$-0.7 \pm 1.4$
$\sigma_+$ ( $\text{m s}^{-1}$ )	0.0	0.0
$\chi^2_\nu$	3.13	1.127
$\sigma_{O-C}$ ( $\text{m s}^{-1}$ )	20.54	5.46
$\overline{\sigma_{RV}}$ ( $\text{m s}^{-1}$ )	11.87	6.15
$\sigma_j$ ( $\text{m s}^{-1}$ )	16.76	$\leq 5.46$
$N_{obs}$	29	23

TABLE 6  
RELATIVE RADIAL VELOCITIES AND BISECTOR SPAN OF BD+15 2940.

Epoch (MJD)	RV ( $\text{m s}^{-1}$ )	$\sigma_{RV}$ ( $\text{m s}^{-1}$ )	BS ( $\text{m s}^{-1}$ )	$\sigma_{BS}$ ( $\text{m s}^{-1}$ )
53452.36375	-46.8	7.8	15.9	17.0
53499.41176	8.4	7.5	5.9	17.8
53844.29702	-40.7	5.5	-4.5	14.5
53866.40534	10.7	6.6	-7.3	18.5
53875.39832	19.5	5.6	-4.7	13.0
53892.16699	37.0	6.3	25.4	16.6
53902.31759	62.6	5.5	1.7	14.9
53910.29146	23.5	5.9	0.3	14.4
53955.16666	-20.7	5.2	-45.9	16.1
53971.13068	-40.3	5.9	-8.1	14.8
54215.25852	-32.1	6.6	28.2	17.0
54225.42513	-27.4	7.9	-15.1	26.1
54248.35726	-29.3	6.1	-36.4	17.1
54276.28661	-6.9	7.6	42.4	19.4
54290.25121	38.6	7.3	-45.6	19.5
54320.17812	37.9	7.6	4.6	20.9
54515.45514	-30.1	7.6	-30.5	19.2
54564.30494	26.3	7.8	-32.5	23.3
54595.22798	47.0	7.7	9.9	17.4
54624.34067	-38.2	7.2	-24.2	16.3
54692.15651	17.6	8.2	25.1	19.1
55018.25340	22.0	8.7	-17.2	17.1
55049.18227	-54.8	6.4	9.2	15.0
55254.40663	28.6	7.8	7.2	20.8
55280.37572	27.5	8.0	34.5	22.8
55582.52001	13.9	7.6	-11.6	20.7
55621.40203	-1.5	7.5	30.7	24.0
55621.41021	-12.4	6.0	16.7	15.0
55674.46852	6.9	7.5	-5.5	18.4
55719.34138	-4.3	6.6	-29.0	15.6
55742.28347	-16.6	6.9	-25.8	15.5
55750.25899	-37.5	7.7	4.4	14.6
55763.22678	-53.9	8.5	-37.6	17.2
55776.18611	-68.1	6.6	-11.2	16.1
55795.13382	-3.2	6.4	-11.2	15.1
55801.11490	35.3	6.1	3.0	15.4
55808.08974	60.0	6.7	-17.4	17.1
55814.09263	43.2	6.3	-18.1	17.5

TABLE 7  
RELATIVE RADIAL VELOCITIES AND BISECTOR SPAN OF HD 233604.

Epoch (MJD)	RV ( $\text{m s}^{-1}$ )	$\sigma_{\text{RV}}$ ( $\text{m s}^{-1}$ )	BS ( $\text{m s}^{-1}$ )	$\sigma_{\text{BS}}$ ( $\text{m s}^{-1}$ )
53015.25986	-28.9	10.6	4.8	26.2
53360.29494	-231.5	10.7	-57.9	22.0
54064.39510	24.8	7.9	43.7	19.3
54136.38069	-172.2	10.6	-2.6	20.6
54208.19384	142.1	9.2	12.1	18.5
54399.46353	135.1	7.5	8.3	20.6
54420.41574	138.1	8.3	5.2	24.2
54500.17910	-193.3	10.0	-50.3	25.1
54564.21884	80.0	9.0	29.2	21.4
54604.14329	119.2	8.5	12.1	20.5
54763.46178	83.8	9.5	-20.0	26.1
54782.43096	193.9	9.0	14.1	28.3
54839.45575	-7.2	10.1	0.1	18.1
54865.19007	-134.9	10.6	15.4	26.7
54891.33472	-183.9	11.9	-7.2	25.9
55173.35355	165.5	9.9	22.4	26.1
55173.37553	159.9	8.6	1.3	24.0
55176.52706	181.0	9.5	64.1	28.6
55214.26133	5.7	9.9	72.5	25.0
55223.20532	-28.9	8.5	36.4	24.8
55254.36068	-151.2	10.3	-43.7	24.1
55307.19447	-102.0	8.1	-10.7	16.1
55486.49435	-145.8	7.5	13.2	21.5
55487.49885	-155.4	6.9	-8.3	18.0
55502.47794	-56.7	9.7	44.5	26.9
55519.38507	18.2	10.6	35.5	30.3
55520.39557	35.2	8.9	-10.1	17.4
55645.26266	-155.3	9.1	49.6	23.1
55659.21377	-190.8	8.2	26.4	15.6
55671.19521	-185.3	7.2	5.7	17.3
55956.18941	167.2	6.9	34.3	17.1
55964.38336	152.6	7.2	3.6	16.4
55971.16102	59.5	7.5	-28.4	15.9

TABLE 8  
ORBITAL PARAMETERS OF BD+15 2940 B AND HD 233604 B.

Parameter	BD+15 2940 b	HD 233604 b
$P$ (days)	$137.48 \pm 0.34$	$192.00 \pm 0.22$
$T_0$ (MJD)	$53464 \pm 16$	$53022 \pm 77$
$K$ ( $\text{m s}^{-1}$ )	$42.7 \pm 4.4$	$177.8 \pm 4.3$
$e$	$0.26 \pm 0.10$	$0.05 \pm 0.03$
$\omega$ (deg)	$302 \pm 33$	$281 \pm 43$
$m \sin i$ ( $M_J$ )	1.11	6.575
$a$ (AU)	0.539	0.747
$RV_0$ ( $\text{m s}^{-1}$ )	$-2.5 \pm 3.3$	$-16.9 \pm 3.7$
$\sigma_+$ ( $\text{m s}^{-1}$ )	18.0	9.0
$\chi^2_\nu$	0.989	2.76
$\sigma_{O-C}$ ( $\text{m s}^{-1}$ )	17.89	19.13
$\overline{\sigma_{\text{RV}}}$ ( $\text{m s}^{-1}$ )	6.97	9.04
$\sigma_j$ ( $\text{m s}^{-1}$ )	16.48	16.86
$N_{\text{obs}}$	38	33

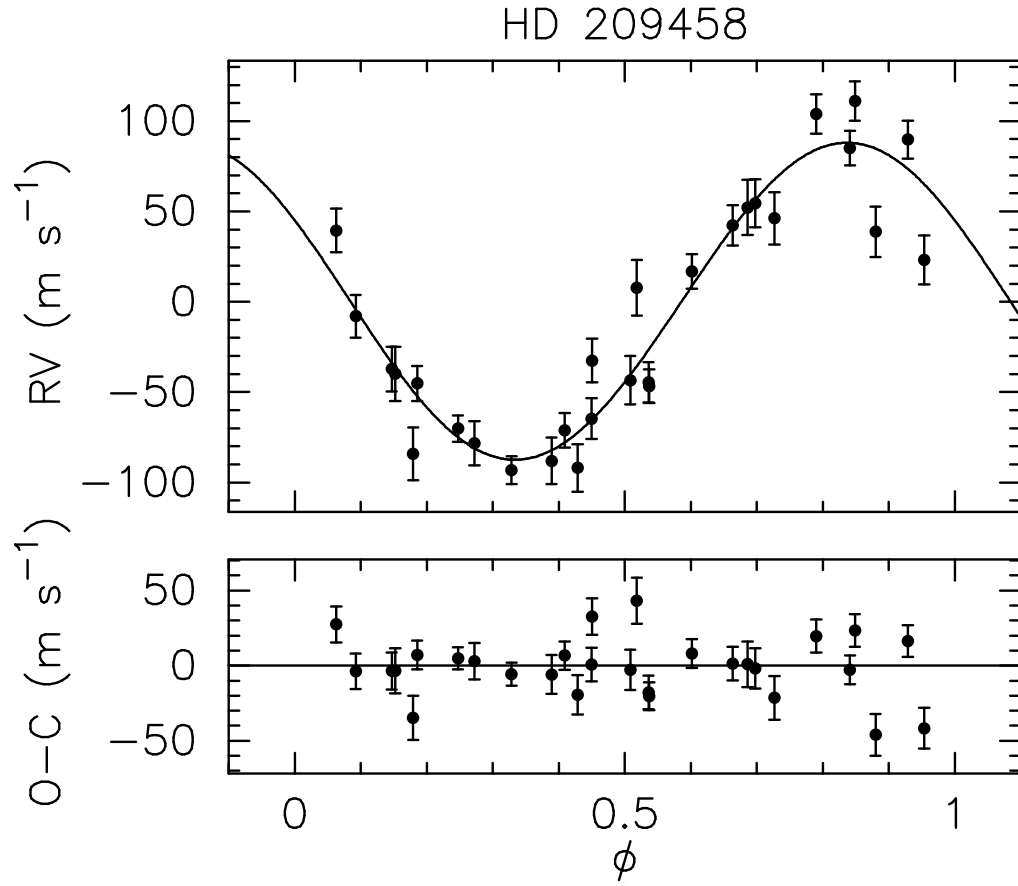


FIG. 1.— Radial velocities of HD 209458 plotted as a function of orbital phase for the solution detailed in Table 5. The measurements taken at or near the transits have been removed.

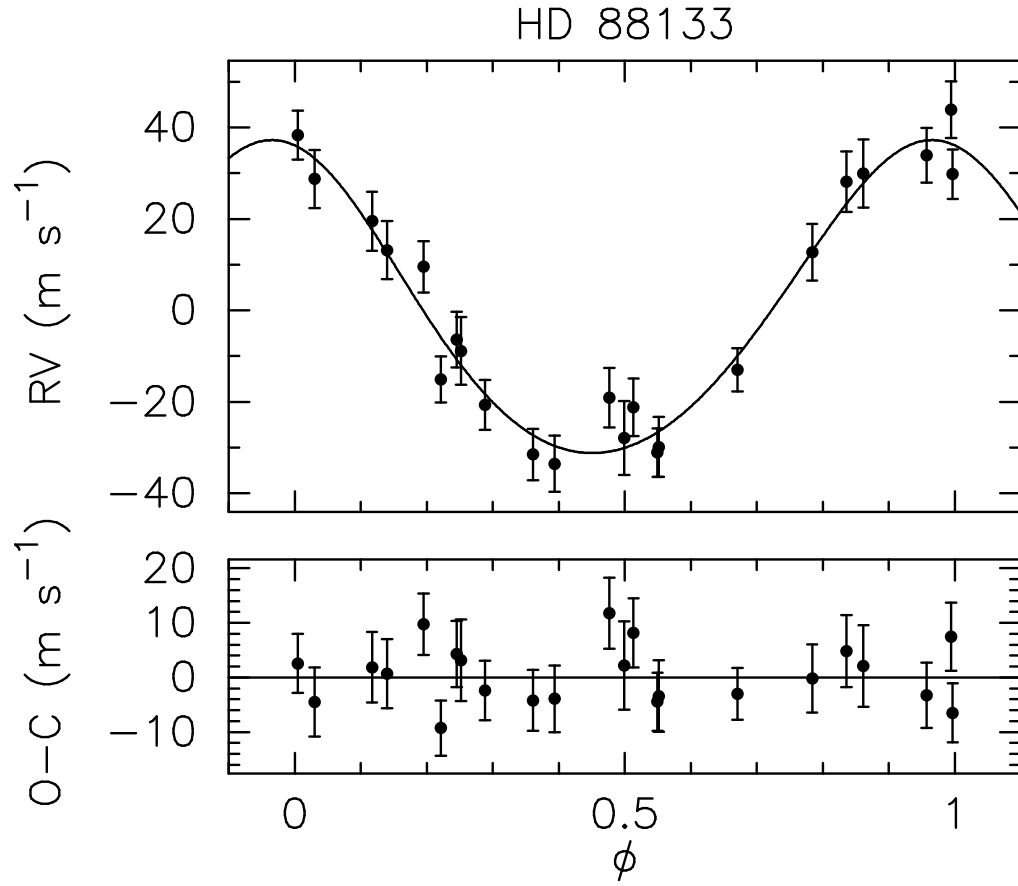


FIG. 2.— Radial velocities of HD 88133 plotted as a function of orbital phase for the solution detailed in Table 5.

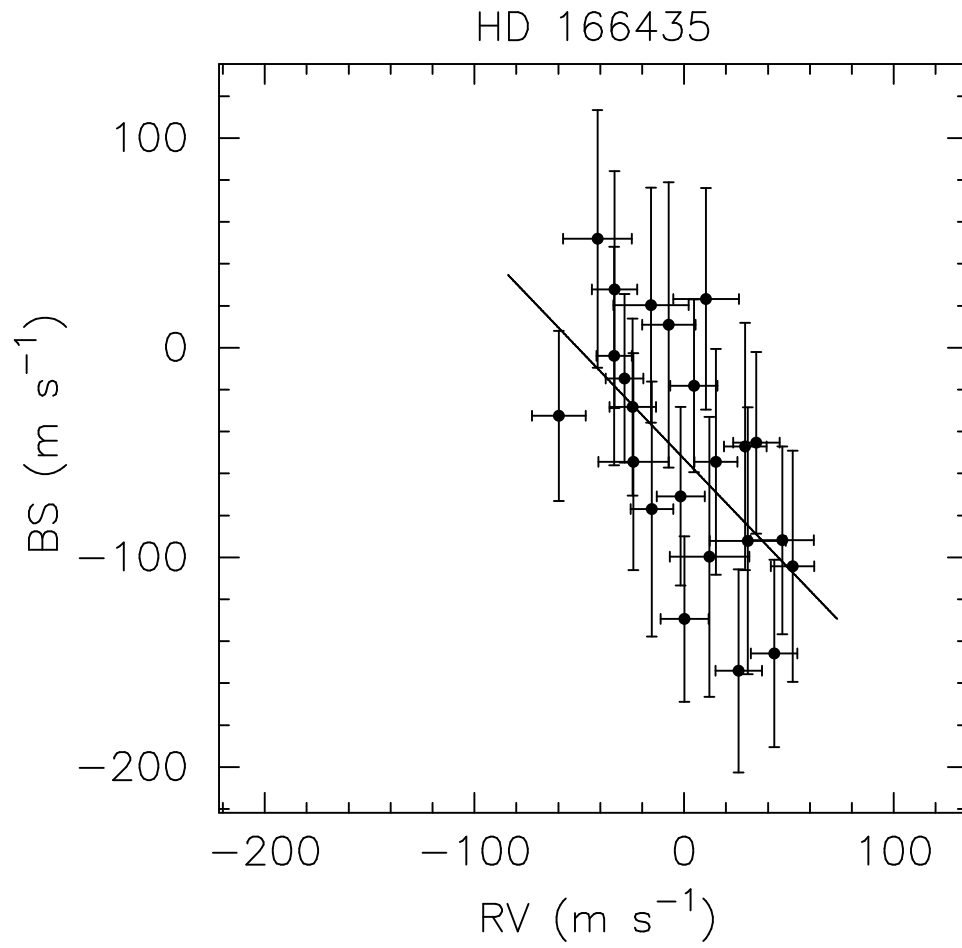


FIG. 3.— Radial velocity versus bisector span of the CCF profile of HD 166435. The line represents the best linear fit to the data.



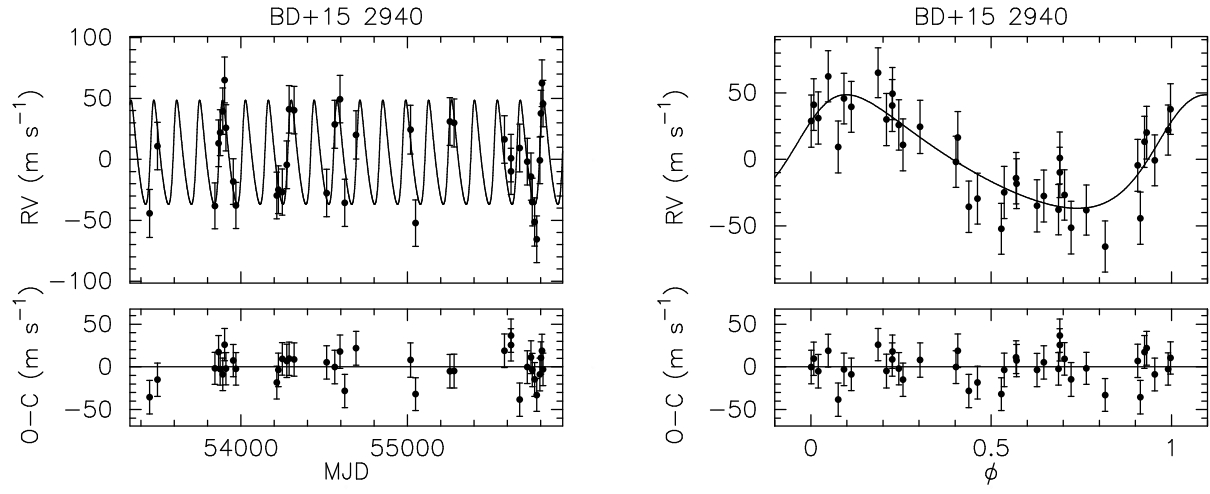


FIG. 4.— Left: radial velocities (filled circles), the best fit Keplerian model detailed in Table 8 (full line) and the post-fit residuals for BD+15 2940. Right: the same as a function of orbital phase.

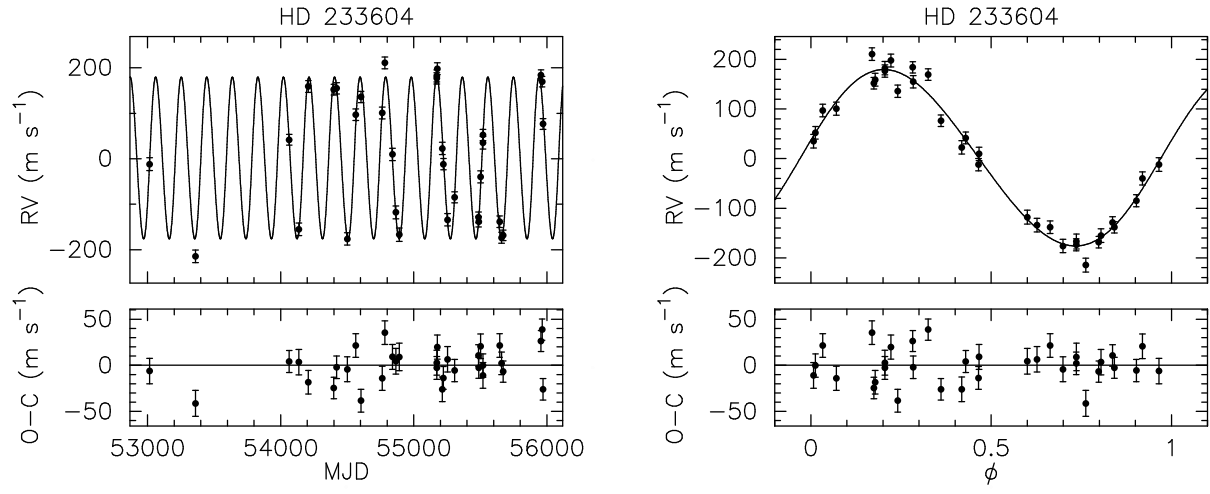


FIG. 5.— Left: radial velocities (filled circles), the best fit Keplerian model detailed in Table 8 (full line) and the post-fit residuals for HD 233604. Right: the same as a function of orbital phase.

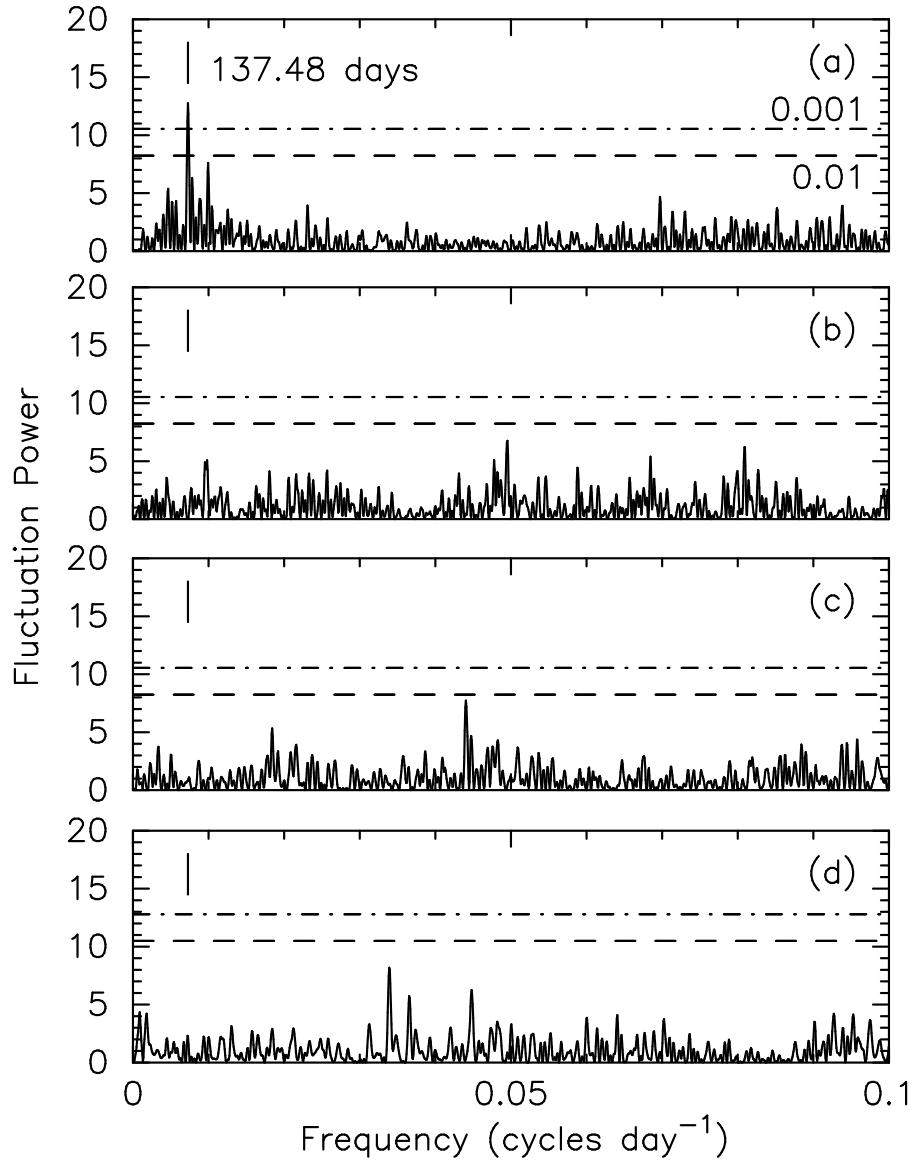


FIG. 6.— The L-S periodograms of (a) radial velocities (b) RV residuals, (c) bisector span and (d) ASAS (Pojmanski 1997) photometry of BD+15 2940. The levels of FAP=1.0% and 0.1% are shown.

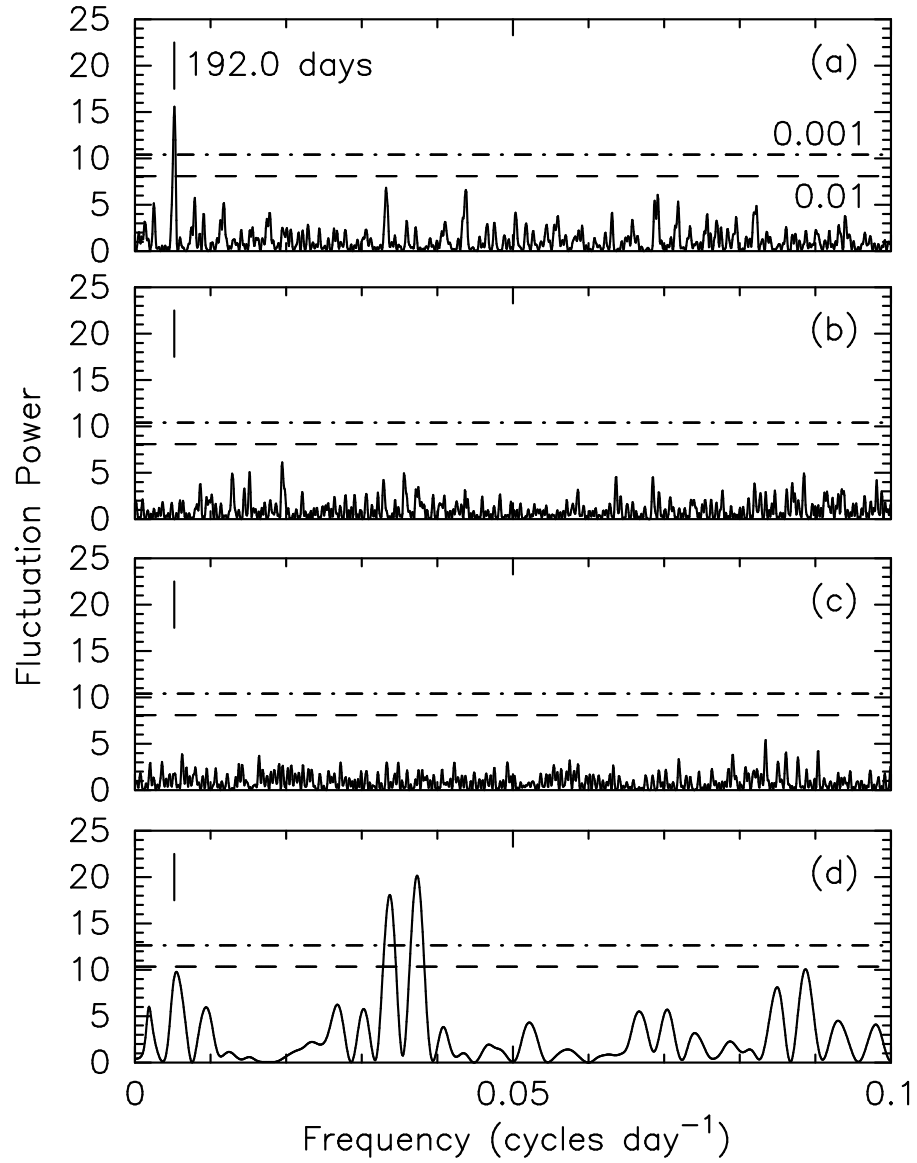


FIG. 7.— The L-S periodograms of (a) radial velocities and their residua (b), (c) bisector span and (d) NSVS (Woźniak et al. 2004) photometry of HD 233604. The levels of FAP=1.0% and 0.1% are shown.

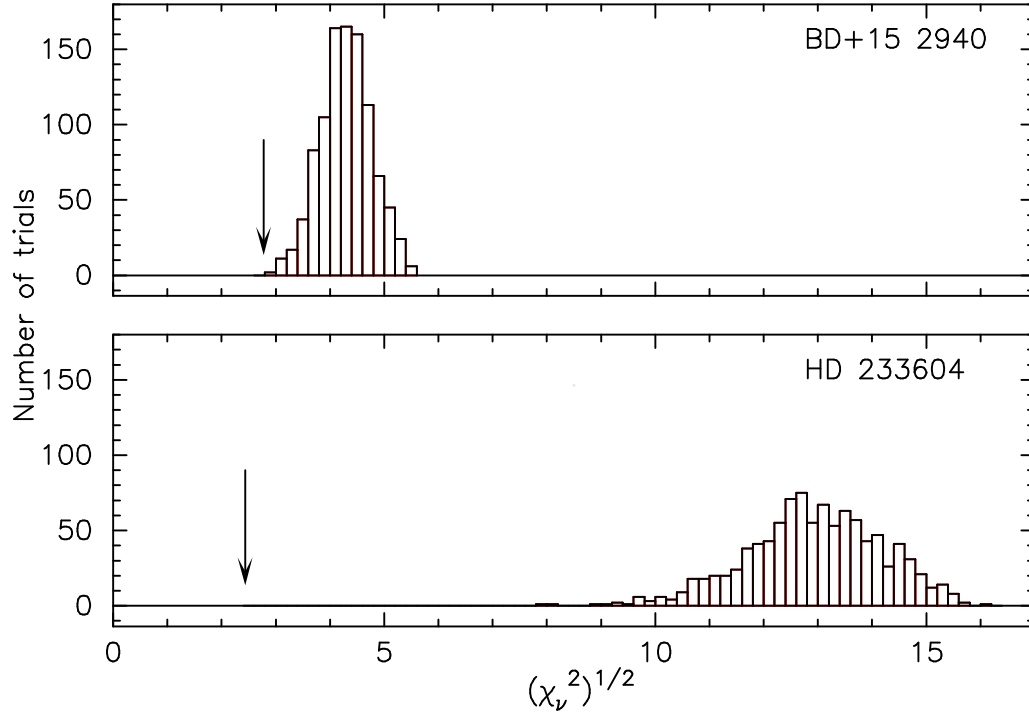


FIG. 8.— Histograms of the values of  $(\chi^2_\nu)^{1/2}$  obtained from the fits of the Keplerian models to scrambled RVs used to estimate the FAPs for the two stars discussed in the text. In each case, 1000 sets of scrambled RVs have been generated. Vertical arrows point to the respective  $(\chi^2_\nu)^{1/2}$  values derived from fits to unscrambled velocities. In both cases the FAP values are less than 0.1%.

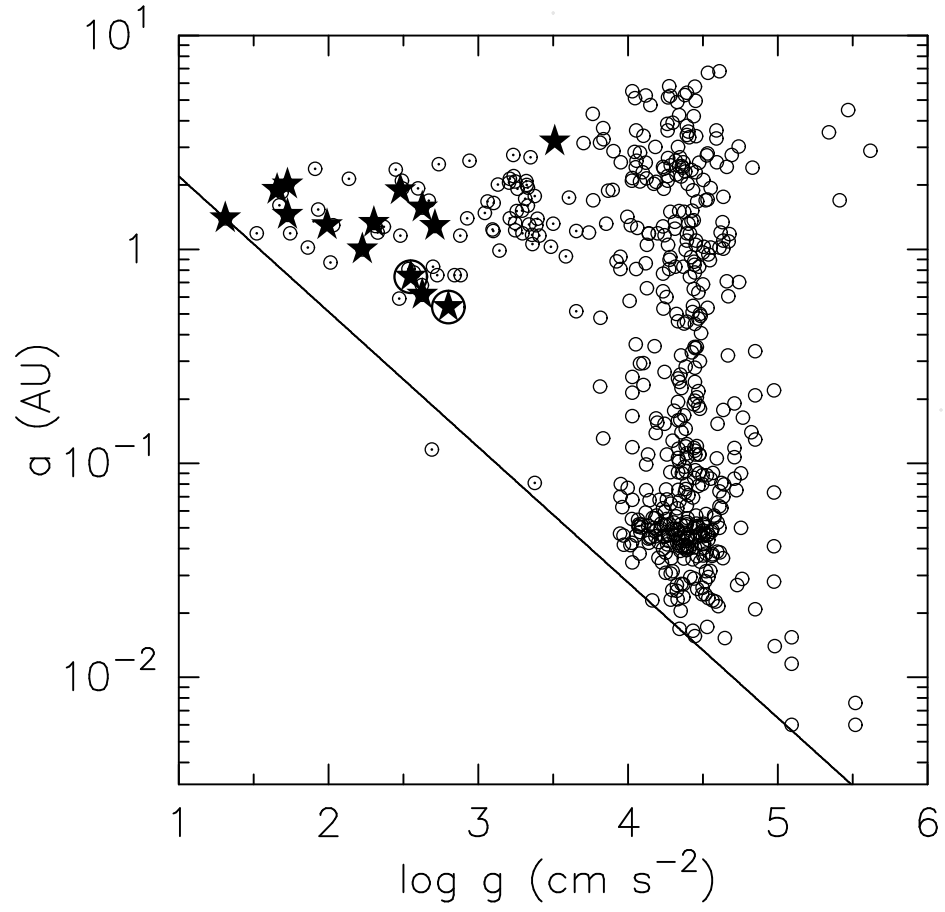


FIG. 9.— Semi-major axes of 778 planets as a function of  $\log g$  of their host stars. The sample of 84 planets orbiting giants and subgiants with  $R_{\star} \geq 3 R_{\odot}$  ( $\odot$ ) includes 12 planets discovered within PTPS survey ( $\star$ ). BD+15 2940 b and HD 233604 b are indicated by  $\star$  with a rim.